Discrimination Between Winter Precipitation Types Based on Explicit Microphysical Modeling of Melting and Refreezing in the Polarimetric Hydrometeor Classification Algorithm

Alexander Ryzhkov[1,2], Heather Reeves[1,2], John Krause[1,2], and Hoyt Burcham[1,2]

[1]*Cooperative Institute for Mesoscale Meteorological Studies, University of Oklahoima, Norman, USA*
[2]*NOAA/OAR/National Severe Storms Laboratory, Norman, USA*
(Dated: 16 July 2014)

1 Introduction

The winter weather Hydrometeor Classification Algorithm (HCA) recently developed at NSSL (Schuur et al. 2012) combines the polarimetric radar data with thermodynamic output from numerical weather prediction models to enhance classification capabilities. The "background classifier" which is based on vertical profiles of temperature and humidity is essential part of HCA. Several existing algorithms for discrimination between four winter precipitation types, snow, rain, freezing rain, and ice pellets / sleet have been tested using a 10-year dataset of soundings and ASOS observations. The results of testing have been summarized in the recent paper by Reeves et al. (2014).

The existing operational NWP models quite poorly describe phase transitions of winter precipitation and generally do not produce reliable discrimination between rain and snow and especially between freezing rain and ice pellets. This is a difficult problem because relatively minor changes in vertical profile of temperature may cause dramatic transformation of dangerous and high-impact freezing rain into relatively harmless form of precipitation consisting of ice pellets or sleet. Fig. 1 shows median vertical profiles of temperature and wet bulb temperature for freezing rain and ice pellets events obtained from a 10-year dataset of soundings and ASOS observations utilized by Reeves et al. (2014). Surface temperatures associated with these two types of precipitation are indistinguishable and the only difference is in the temperature of elevated inversion which is about 2° higher for freezing rain.

One of the major deficiencies of the models with bulk microphysics is inadequate treatment of the processes of melting and refreezing of hydrometeors. Even the most sophisticated models use primarily the vertical profiles of temperature and humidity to identify "warm" atmospheric layers where melting of snowflakes occurs and "cold" layers where completely or partially melted snowflakes undergo refreezing. The degree of melting / refreezing crucially depends on the residence time of the particles in such layers. The residence times vary dramatically depending on the terminal velocity of hydrometeors which is a strong function of particle size, density, shape, and phase composition. The models with bulk microphysics essentially ignore such dependencies.

The most common atmospheric stratification favoring freezing rain and /or ice pellets / sleet is characterized by the temperature inversion with positive temperature aloft and the cold subfreezing layer beneath next to the surface. Under such scenario, dry snowflakes melt either completely or partially in the elevated melting layer and then may refreeze in the cold surface layer. Partially melted snowflakes start refreezing instantaneously while they fall into the subfreezing layer. Completely melted snowflakes (rain or drizzle particles) may not refreeze in the cold layer because they have to nucleate first which requires even colder temperature at which ice nuclei inside them become active. This very important difference in the behavior of completely melted and partially melted snowflakes is ignored in the operational models as well.

In this study, a principally new "background classifier" based on 1D model of melting / refreezing with spectral microphysics has been developed and validated on the dataset which is used by Reeves et al. (2014).

2 Model description

A simple one-dimensional model with spectral (bin) microphysics is suggested which explicitly treats the processes of melting / refreezing by taking into account the initial size distribution and density of dry snowflakes and describes the evolution of mass water fraction and density of hydrometeors as they fall to the ground separately in 80 size bins. The model quantifies mixing ratios and precipitation rates associated with liquid and solid parts of precipitation for a given size distribution and density of dry snowflakes above the melting layer. Hence the model is capable to identify the dominant type of precipitation at the surface and to estimate relative proportions of liquid and solid precipitation in the mixture. The model assumes no interactions between particles such as riming or aggregation. In other words, one snowflake aloft produces a single (generally mixed-phase) particle at the surface.

The required model inputs include vertical profiles of temperature, relative humidity, and pressure. The model prescribes initial size distribution of snowflakes at the top of the domain at subfreezing level above the melting layer and the degree of riming of snowflakes. It is assumed that snow density decreases with size following Brandes et al. (2007) and decreases with the degree of riming. The assumptions pertaining to the size distribution and the degree of riming can be based on the

polarimetric radar data. Our simulations indicate that the choice of the initial size distribution of snowflakes does not affect much the prevalent type of precipitation on the ground but it is important for quantifying precipitation amount at the surface.

Standard heat balance equations describing the processes of melting and refreezing (e.g., Szyrmer and Zawadzki 1999; Zawadzki et al. 2005; Kumjian et al. 2012) are solved to obtain vertical profiles of mass water fraction separately for every size bin. An example of such profiles for particles with different melted diameters is presented in Fig. 2. Vertical profile of temperature with well pronounced warm elevated layer is indicated in the left panel of Fig. 2. Our model shows that snowflakes with melted diameter of 1 and 2 mm are melted completely within the melting layer (right panel of Fig. 2). The model assumes that the ice nucleation temperature is -5°C and all raindrops originated from completely melted snowflakes start refreezing regardless of their size at temperatures below -5°C. Liquid drop with melted diameter of 1 mm refreezes completely within the subfreezing surface layer in this example while a 2-mm drop refreezes only partially. Snowflakes with melted diameters of 3, 4, and 5 mm do not melt completely within the melting layer and start refreezing immediately at negative temperatures because they do not need ice nucleation. All these particles refreeze only partially and contain both liquid and solid parts when they reach the surface.

3 Vertical profiles of radar variables

Vertical profiles of mass water fraction have been used to compute vertical profiles of radar variables such as radar reflectivity Z, differential reflectivity Z_{DR}, and specific differential phase K_{DP} using the forward radar observation operator described in Ryzhkov et al. (2011). Polarimetric variables depend on particle shape, orientation, density, and phase composition of hydrometeors which were explicitly determined as functions of mass water fraction as prescribed by Ryzhkov et al. (2011). Vertical dependencies of Z, Z_{DR}, and K_{DP} at S band have been determined for typical temperature profiles conducive for freezing rain (Fig. 3) and ice pellets (Fig. 4). The melting layer signature aloft is clearly exhibited in both cases. However, in the case of dominant ice pellets another notable polarimetric signatures, namely, sharp peaks in the Z_{DR} and K_{DP} profiles show up at the level where ice nucleation with subsequent refreezing starts (Fig. 4). This is a so called "refreezing signature" which was recently discovered in multiple polarimetric radar observations (Kumjian et al. 2013). Typical vertical profiles of Z, Z_{DR}, K_{DP}, and ρ_{hv} at S band measured in the presence of refreezing are displayed in Fig. 5 (Kumjian et al. 2013).

Kumjian et al. (2013) consider two possible underlying mechanisms for the "refreezing signature". One of them is similar to what happens during evaporation of raindrops (Kumjian and Ryzhkov 2010). Smaller raindrops evaporate first and resulting Z_{DR} increases due to enhanced contribution from larger raindrops which have higher intrinsic Z_{DR}. In the case of refreezing, smaller liquid drops refreeze first but, as opposed to the case of evaporation, they are not eliminated from the size spectrum. Instead, their reflectivity drops by about 7 dB due to the transition of water to ice, and therefore, their relative contribution to Z_{DR} diminishes compared to larger partially frozen raindrops. Another possible mechanism discussed in Kumjian et al. (2013) is local generation of highly anisotropic ice crystals at the level of ice nucleation which may boost Z_{DR}. The fact that our model which does not consider local generation of ice crystals reproduces realistically looking refreezing signatures testifies that the first mechanism is probably dominant and is more likely explanation of the phenomenon.

4 Validation of the background classifier

The background classifier utilizes vertical profiles of temperature and humidity (or wet bulb temperature) to discriminate between 4 major precipitation types near the surface: rain (RA), snow (SN), freezing rain (FZR), and ice pellets / sleet (IP). Snow can be subdivided into dry and wet snow and the mixture of FZR and IP can be also identified as a separate class. The classifier was validated using the same dataset of soundings and ASOS observations which was utilized in the Reeves et al. (2014) study. It includes a 10-year record of soundings at a number of US locations where surface temperature was hovering around 0°C and transitional winter precipitation of various types was observed and well documented. 1741 events associated with snow (649), rain (545), ice pellets (125), and freezing rain (422) were examined. We compare the performance of the new classifier (NSSL2) with five classification algorithms analyzed by Reeves et al. (2014): Baldwin 1 and 2 (Baldwin 1994), Bourgouin (2000), Ramer (1993) and NSSL1 (Schuur et al. 2012).

The most recent NSSL2 scheme which involves explicit treatment of the processes of melting and refreezing demonstrates the best performance (Table 1). The NSSL2 scheme quantifies the ratio of liquid and solid precipitation rates. It also identifies wet snow in a broader category of snow. Hit rates for IP and FZR are very close to each other for NSSL2 as opposed to other algorithms except Bg which has lower hit rates for both classes. In our simulations, we varied ice nucleation temperature and found that -5°C yields the best results which are listed in Table 1.

5 Combining model and radar data

Once background classification is made, the radar information is utilized either to confirm or reject the results of background classification in the areas of radar echo. The focus is on reliable identification of the melting layer in the radar data. If the storm is deep enough and the melting layer is clearly identified, then one can be mode confident that a "classical" mechanism for producing freezing rain or ice pellets is at work. It is known that freezing drizzle / rain can be generated without melting layer recognized in the radar data. This is a so called "supercooled warm rain process" when drizzle is

produced at subfreezing temperatures next to the surface and is not converted to ice if air temperature is above the nucleation temperature of ice. Our background classifier does not work under this scenario.

Table 1. Hit rates of different background classifiers

	SN	RA	IP	FZR
B1	87.7	96.1	89.6	28.4
B2	97.1	96.1	56.0	28.4
Bg	92.6	96.1	50.4 / 60.0	48.8 / 55.7
Ra	94.9	99.6	25.6	65.4 / 66.1
NSSL1	94.1	96.4	26.4 / 70.4	40.3 / 78.9
NSSL2	89 / 98	100	59 / 75	61 / 80

B1 and B2 – Baldwin 1, 2 (1994), Bg – Bourgouin (2000), Ra – Ramer (1993), NSSL1 – Schuur et al. (2012). Second values in Table 1 correspond to the hit rate if IP/FZR is considered a hit.

Positive correlation between Z_{DR} and Z at low altitudes below the melting layer is a manifestation of rain or freezing rain. No such correlation is expected in the case of ice pellets and inverse dependence of Z_{DR} on Z is an indication of dry aggregated snow.

As mentioned before, radar measurements can be used to optimize the parameters of initial snow size distribution aloft and to roughly estimate the degree of snow riming. A large dataset of raindrop size distributions measured in central Oklahoma is utilized for choosing an appropriate size distribution of melted snowflake diameters based on the value of radar reflectivity in rain at the surface. The dataset contains 47144 raindrop size distributions measured over the period of 7 years (Schuur et al. 2005). The median size distributions have been estimated for different reflectivity values (Fig. 3). The corresponding size distributions of snowflakes have been retrieved assuming the conservation of the flux of particles through the transition from snow to rain (Fig. 4) (Zhang et al. 2011). The size distributions of snowflakes are obtained assuming different degrees of riming of snow f_{rim} (dashed curves are for $f_{rim} = 1$, dash-dotted curves are for $f_{rim} = 5$). Measurements of Z_{DR} above the freezing level and polarimetic properties of the melting layer can be used for rough estimate of $f_{rim.}$ Z_{DR} in snow usually decreases with increasing f_{rim} and downward excursion of the ML signatures testifies that snow aloft is rimed.

6 Conclusions

A new algorithm for "background" classification of different types of winter precipitation at the surface including snow, rain, freezing rain, and ice pellets has been developed. The algorithm uses vertical profiles of temperature, humidity, and pressure retrieved from the NWP model and utilizes polarimetric radar data for retrieving initial size distribution of snowflakes above the freezing level. This is a spectral (bin) model which treats the processes of melting and refreezing separately for each size bin. The consistency of model data with radar data serves as feasibility check of the "background" classifier performance.

The cloud model after conversion to the fields of polarimetric data is capable to reproduce the "refreezing" signature in the case of ice pellets which is manifested by local maximum of Z_{DR} and K_{DP}.

The model was validated using a 10-year dataset of soundings and ASOS observations. It is shown that the new classifier outperformed all other existing algorithms listed in Reeves et al. (2014).

References

Baldwin, M., R. Treadon, and S. Contorno, 1994: Precipitation type prediction using a decision tree approach with NMCs mesoscale eta model. Preprints. *19th Conf. on Numerical Weather Prediction*, Portland, OR, Amer. Meteor. Soc., 30 – 31.

Bourgouin, B., 2000: A method to determine precipitation type. *Wea. Forecasting*, 15, 583 – 592.

Brandes, E., K. Ikeda, G. Zhang, M. Schoenhuber, and R. Rasmussen, 2007: A statistical and physical description of hydrometeor distributions in Colorado snowstorms using a video-disdrometer. *J. Appl. Meteor.*, **46**, 634 – 650.

Kumjian, M. and A. Ryzhkov, 2010: The impact of evaporation on polarimetric characteristics of rain. Theoretical model and practical implications. *J. Appl. Meteor. Clim.*, **49**, 1247 – 1267.

Kumjian, M., S. Ganson, and A. Ryzhkov, 2012: Freezing of raindrops in deep convective storms: A microphysical and polarimetric model. *J. Atmos. Sci*., **69**, 3471 – 3490.

Kumjian, M., A. Ryzhkov, H. Reeves, and T. Schuur, 2013: Dual-polarization radar observations of hydrometeor refreezing in winter storms. *J. Appl. Meteor. Clim.*, **52**, 2549 – 2566.

Ramer, J., 1993: An empirical technique for diagnosing precipitation type from model output. Preprints. Fifth Int. Conf. on Aviation Weather Systems. Vienna, VA, Amer. Meteor. Soc., 227 – 230.

Reeves, H., K. Elmore, A. Ryzhkov, T. Schuur, and J. Krause, 2014: Sources of uncertainty in precipitation types forecasting. *Wea. Forecasting*, **29**, 936 – 953.

Ryzhkov, A., M. Pinsky, A. Pokrovsky, and A. Khain, 2011: Polarimetric radar observation operator for a cloud model with spectral microphysics. *J. Appl. Meteor. Clim.*, **50**, 873 – 894.

Schuur, T.J., A.V. Ryzhkov, and D.R. Clabo, 2005: Climatological analysis of DSDs in Oklahoma as revealed by 2D-video disdrometer and polarimetric WSR-88D. Preprints, *32nd Conference on Radar Meteorology*., CD-ROM, 15R.4

Schuur, T., H.-S. Park, A. Ryzhkov, and H. Reeves, 2012: Classification of precipitation types during transitional winter weather using the RUC model and polarimetric radar retrievals. *J. Appl. Meteor. Clim.*, **51**, 763 – 779.

Szyrmer, W., and I. Zawadzki, 1999: Modeling of the melting layer. Part I: Dynamics and microphysics. *J. Atmos. Sci.*, **56**, 3573 – 3592.

Zawadzki, I., W. Szyrmer, C. Bell, and F. Fabry, 2005: Modeling of the melting layer. Part III: The density effect. *J. Atmos. Sci.*, **62**, 3705 – 3723.

Zhang, G., S. Luchs, A. Ryzhkov, M. Xue, L. Ryzhkova, Q. Cao, 2011: Winter precipitation microphysics characterized by polarimetric radar and video disdrometer observations in central Oklahoma. *J. Appl. Meteor. Clim.*, **50**, 1558 – 1570.

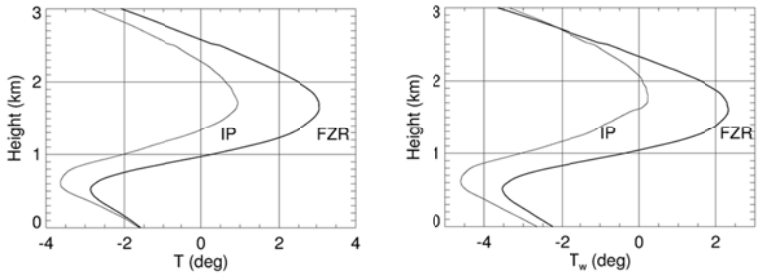

Fig. 1. Median profiles of temperature (left panels) and wet bulb temperature (right panels) for freezing rain (FZR) and ice pellets (IP).

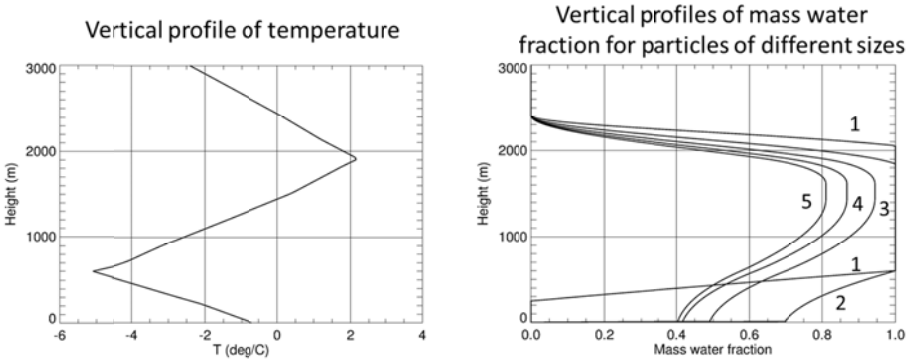

Fig. 2. Simulated profiles of mass water fraction for particles with different melted diameters (marked with numbers equal to melted diameters expressed in mm) for the vertical profile of temperature shown in left panel.

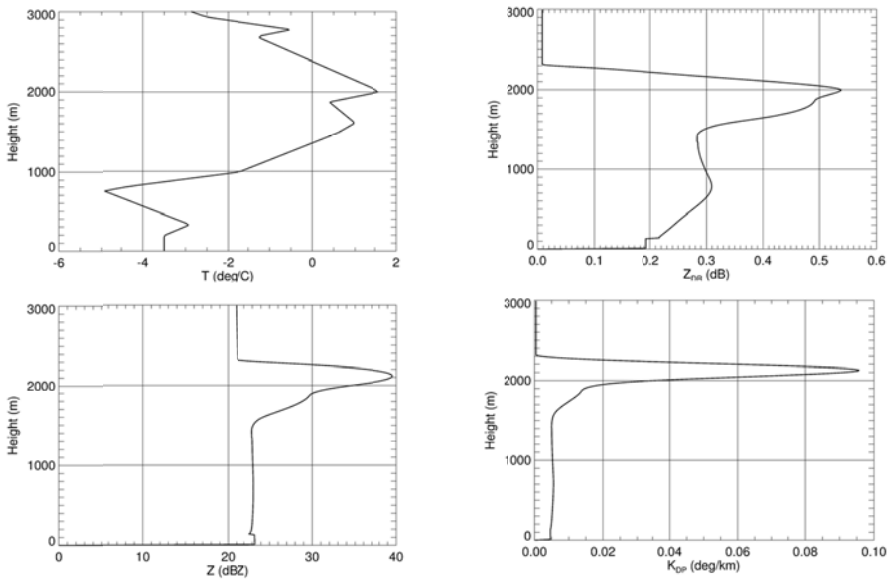

Fig. 3. Vertical profiles of radar variables and temperature for the case of freezing rain at the surface.

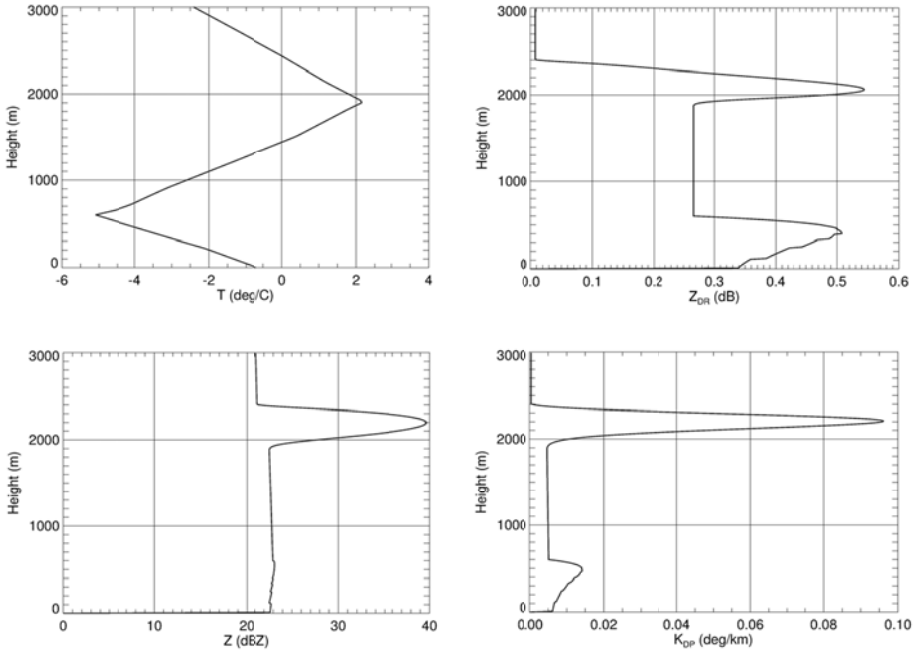

Fig. 4. Same as in Fig. 3 but for the case with ice pellets on the surface.

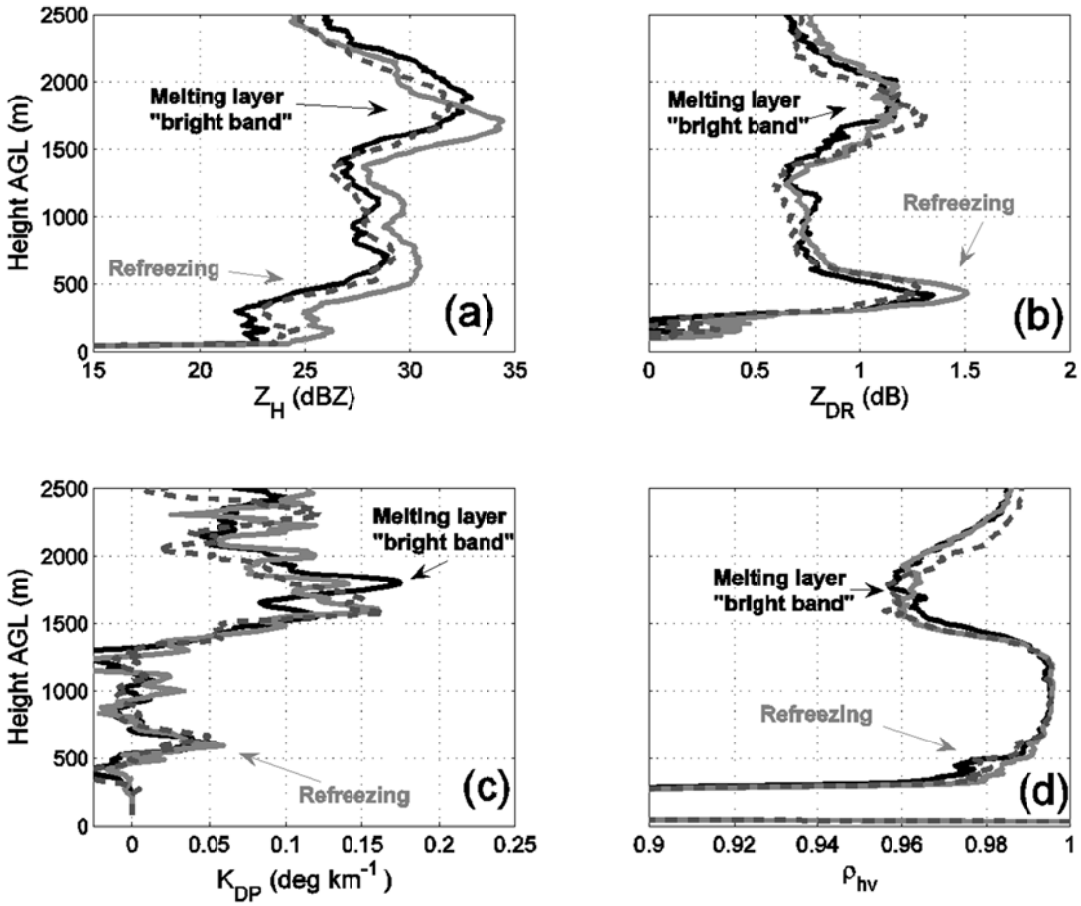

Fig. 5. Observed vertical profiles of Z, Z_{DR}, K_{DP}, and ρ_{hv} in the case of refreezing. Adapted from Kumjian et al. (2013).

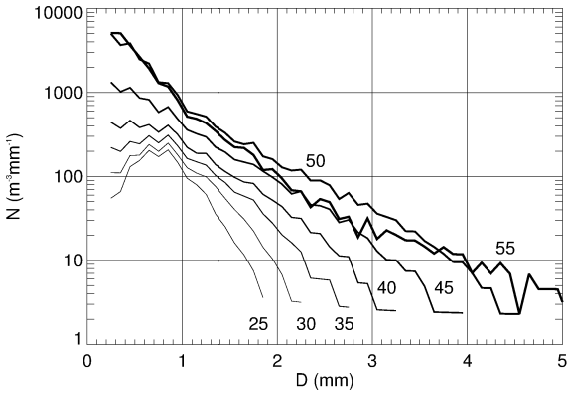

Fig. 6. Median DSDs in rain for different radar reflectivities estimated from large Oklahoma disdrometer dataset.

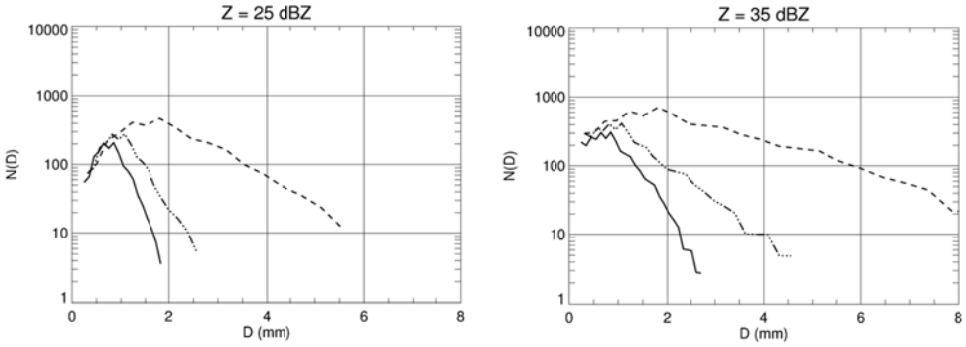

Fig. 7. Raindrop size distributions (solid lines) and the corresponding size distributions of snowflakes for unrimed (f_{rim} = 1) (dashed lines) and heavily rimed (f_{rim} = 5) (dash-dotted lines) snow aloft for the radar reflectivities in rain at the surface equal to 25 and 35 dBZ.